Chemical Research in Toxicology

ARTICLE

pubs.acs.org/crt

Studies of Intracorneal Distribution and Cytotoxicity of Quantum Dots: Risk Assessment of Eye Exposure

Tsung-Rong Kuo,[†] Chia-Feng Lee,[†] Sung-Jan Lin,[‡,§] Chen-Yuan Dong,[∥] Chia-Chun Chen,[*,†,⊥] and Hsin-Yuan Tan[*,‡,#]

[†]Department of Chemistry, National Taiwan Normal University, Taipei, Taiwan

[‡]Institute of Biomedical Engineering, College of Medicine and Engineering, National Taiwan University, Taipei, Taiwan

[§]Department of Dermatology, National Taiwan University Hospital, Taipei, Taiwan

[∥]Department of Physics, National Taiwan University, Taipei, Taiwan

[⊥]Institute of Atomic and Molecular Sciences, Academia Sinica, Taipei, Taiwan

[#]Department of Ophthalmology, Chang Gung Memorial Hospital, College of Medicine, Chang Gung University, TaoYuan, Taiwan

ABSTRACT: The cornea is a potential route of exposure and drug administration for nanoparticles. In this work, we use noninvasive two-photon microscopic imaging to study the distribution and permeability pathway of CdSe/ZnS core/shell quantum dots (QDs) capped with three different functional groups through the cornea. With no additional staining, the two-photon image clearly discloses that fluorescent QDs penetrate and reside within the interlamellar space of second harmonic generating collagenous stroma when the corneal epithelium barrier is injured. An in vitro cytotoxicity test using bovine corneal stromal cells incubated individually with all three kinds of QDs indicates that the cell viability decreases significantly as the QD concentration and incubation period increased. The results also show that the specific QDs influence corneal stromal cell viability up to a significant magnitude of 50% under a relatively low concentration (5−20 nM) and short exposure period (24−48 h). Furthermore, two-photon imaging shows that QDs can be retained within the cornea up to 26 days in an in vivo mouse model. On the basis of our in vivo and in vitro data, we conclude that QDs can penetrate and be retained within cornea long enough to cause consequential cytotoxicity, under the circumstance in which the corneal epithelium barrier is injured. Since corneal abrasion is quite a common situation in daily life, our work raises public attention to the potential risk of eye exposure to nanoparticles.

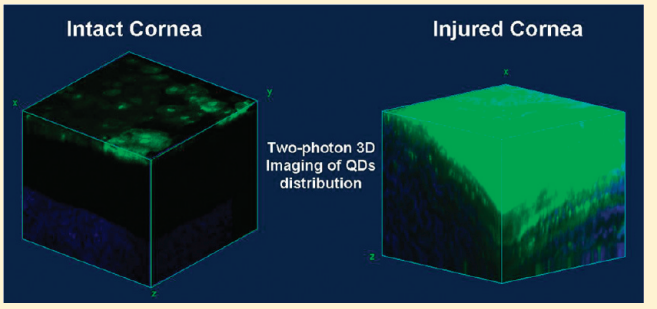

INTRODUCTION

The possibility of nanoparticle exposure in daily life has increased recently as the emerging incorporation of nanotechnology into various consumer products, such as cosmetics and electronics, becomes quite popular. Despite a number of works that have aimed at evaluating the health effects of nanoparticles, the conclusion of the potentials of nanotoxicity is still equivocal.[1−5] Take core/shell CdSe/ZnS quantum dots (QDs) for example; they are one of the most commonly applied nanoparticles, and the chance of exposure at an occupational scenario is relatively high since they have been widely introduced into the field of biomedicine, and significant advances have been made in biological applications including imaging, assay, and drug delivery for years.[6−17] Recenty, a number of studies addressing QD cytotoxicity have indicated that QDs with specific surface coating groups, compositions, and sizes may be quite cytotoxic in various cell types.[18−21] Also, several in vivo studies have documented the possibility of unintended bioaccumulation of QDs which may thereby imply the potential consequential toxicity for animal health.[22−25] A previous article by Lewinski et al. has summarized recent works regarding the issue of the cytotoxicity of nanoparticles, including QDs, which discloses the wide variety of experimental parameters that made the conclusions incomparable.[1] Theoretically, the potential routes of administration, the risks for exposure, and the possible toxicity should be addressed cautiously to ensure experimental and clinical safety. Moreover, an understanding of possible interactions of QDs within human tissues may shed light on the prevention of health risks in the laboratory and daily exposure to nanoparticle-containing merchandise.

Many different routes of administration and exposure of QDs have been discussed.[26,27] Intravenous injection is a major route for drug administration. It has been reported that intravenously injected QDs may accumulate in unintended tissues, which implied

Received: November 8, 2010
Published: January 24, 2011

that the potential toxicity may result from the failure of clearance from the body.[28] The possibility of tissue uptake of QDs via ingestion following exposure has also been proposed in animal and cell culture models.[27,29−31] Skin is another important portal of entry for nanoparticles in occupational scenarios and also a potential route of systemic drug administration.[32−35] QDs with various physicochemical properties have been demonstrated to penetrate the intact stratum corneum barrier 8 h following topical applications.[36] In addition, intradermal injection of QDs in a mice model may result in QD migration to sentinel organs.[37] The cornea is another common route of drug administration and also an important route of nanoparticle exposure in occupational scenarios and daily life. However, the possibility of QD penetration into the cornea has not been discussed before.

The potential cytotoxicity of QDs is another important issue to be verified before clinical applications. Several in vivo and in vitro reports have indicated that QDs may be internalized and affect cell viability in variable degrees in different cell types, while the effect was proposed to be related highly to both the inherent physicochemical properties and environmental conditions.[38−41] Jaiswal et al. demonstrated that targeted CdSe/ZnS QDs could be internalized by HeLa cells and retained within live cells for more than 10 days with no significant effect on cell viability.[42] Dubertret et al. injected micelle-encapsulated CdSe/ZnS QDs into *Xenopus* embryos and found a growth pattern similar to that of the control under the dosage of 2×10^9/cell.[43] In vivo QD deposition within tissue via intravenous injection was observed in both rat and mice models with no sign of QD breakdown up to a month. Hanaki et al. showed that MUA-coated QDs could stay in Vero cells without inducing cytotoxicity under the concentration of 0.4 mg/mL,[44] and Shiohara et al. has further pointed out a concentration-dependent effect using a similar experimental system.[45] In addition to the dose-dependent cytotoxic effect shown by several different cell types, surface coating of QDs can affect cytotoxicity. The ZnS shell has been proven to be effective in reducing the cytotoxic effect from releasing the free cadmium ion of QDs in the rat primary hepatocytes culturing system,[46] while Selvan et al. proposed a better protective effect by SiO_2 coating than ZnS coating, while the effect was also dose-dependent.[47] Kirchner et al. has further pointed out the correlation between cellular uptake and the cytotoxic effect among different surface coatings: the lower the uptake for PEG-coating, the lower cytotoxicity.[48] A similar effect has also been shown in primary human epidermal keratinocyte culturing systems.[49] Pro-inflammatory cytokine increased after carboxylic acid coated QD exposure but not with PEG-coated QDs. The cytotoxic effect became apparent by 48 h at the highest concentration of 20 nM, which was also shown be time- and dose-dependent. However, while surface coating and extracellular dosage were proven to affect the cytotoxic effect of QDs, Chang et al. have demonstrated the similarity of cytotoxicity among different surface coating QDs when their intracellular concentration of QDs was the same, which suggests that the effect depended more on the intracellular concentration.[29]

Two-photon microscopy has advantages of improved penetration depth, reduced photobleaching, and capability for optical sectioning. The technique is feasible for cornea imaging.[50−53] Two-photon excited autofluorescence and second harmonic generation (SHG) signals derived from collagenous stroma outline the architecture of the cornea with no need for additional processing. QDs were also proven to exhibit very bright and stable fluorescence in vivo using two-photon excitation. Here, we attempt to use this noninvasive imaging system to investigate the permeability of the cornea, another important route of entry for nanoparticles, to the untargeted QDs, and the biodistribution of QDs within cornea. Also, we study the interactions of corneal stromal cells with QDs and the parameters that might affect cell viability.

EXPERIMENTAL PROCEDURES

QDs Capped with Different Functional Groups. The QDs of core/shell CdSe/ZnS nanocrystals with emission maxima at 565 nm (QD565) and 655 nm (QD655) were purchased from Invitrogen (Hayward, CA). QD565 was spherical, with an outside diameter of 4.6 nm, and QD655 was ellipsoid (6 nm × 12 nm). The QDs of each size were coated individually with polyethylene glycol, amines, and carboxylic acids to form QD-PEG, QD-NH_2, and QD-COOH, respectively. The resulting samples were neutral (QD-PEG, pH 8.3), positive (QD-NH_2, pH 8.3), and negative (QD-COOH, pH 9.0) as supplied in a 50 mM borate buffer.

Bovine Cornea Incubated with QDs for Two-photon Microscopy Imaging. Freshly derived bovine corneas (intact with epithelium and removed from epithelium) were mounted in vertical Franz diffusion cells. The acceptor chambers of the Franz diffusion cells were filled with PBS, and the donor chambers were filled with different QD solutions. Bovine cornea was incubated with QD solutions individually for 30, 60, and 80 min and 3 h. After incubation, the sample was used for the studies of the permeability of QDs.

A home-built two-photon microscopic system was applied to noninvasive corneal imaging.[35,54] The two-photon microscope based on a commercial upright microscope (E800, Nikon, Japan) was used in this study. The excitation source was a titanium-sapphire pulse laser (Tsunami, Spectra Physics, Mountain View, CA) pumped by a diode pump (Millennia X, Spectra Physics, Mountain View, CA). The 780-nm output of the titanium-sapphire laser was used in our experiments. Upon reflection by the short-pass, the main dichroic mirror (700dcspruv-3p, Chroma Technology, Rockingham, VT), the circularly polarized laser source was then focused by an oil-immersion objective (S Fluor, NA 1.3, Nikon, Melville, NY). After the signals were generated, fluorescence and SHG were separated by a secondary dichroic mirror (435 dcxr, Chroma Technology) and filtered, separately, by two band-pass filters (MF: E435lp-700sp, SHG: HQ390/20, Chroma Technology) for the respective detection of fluorescence (435 to 700 nm) and SHG signals (380 to 400 nm). Single-photon counting photomultiplier tubes (R7400P, Hamamatsu, Japan) were used as the detector.

In Vivo Intrastromal QD Injection in the Mice Model. The mice used in this study were humanely treated in accordance with the ARVO resolution on the use of animals in research. C57BL/6J mice were anesthetized for intrastromal injection. The QD565-COOH solution (10 μL, 4 μM, [CdSe] = 1 mM) was injected into one eye of the mouse. For comparison, 10 μL of PBS was then injected into the other eye of the same mouse. After 26 days, the mouse was euthanized, and fresh eyeball samples were harvested for two-photon imaging in order to investigate the possible intracorneal accumulation of QDs.

Cell Culture and QDs Treatment for BCF and BSF. The corneas of fresh bovine eyeballs were removed, and then bovine corneal fibroblasts (BCF) were isolated from corneal buttons using collagenase digestion methods. Bovine skin fibroblasts (BSF) were derived and cultured from explants of freshly harvested bovine skin. The fibroblasts were then cultured in Dulbecco's modified Eagle's medium (DMEM) supplemented with 10% fetal bovine serum. Before QD treatment, the BCF and BSF were seeded at a density of 5×10^4 cells/cm^2 onto a 24-well plate and were grown for 1 day. The medium in the 24-well plate was replaced with only DMEM- or DMEM-containing QDs. The final molar concentrations of QDs were controlled to be 5, 10, and 20 nM

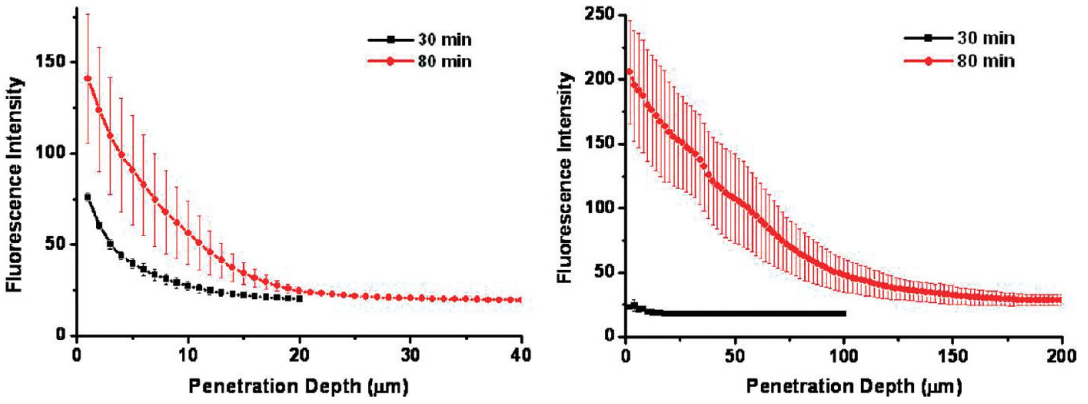

Figure 1. Fluorescent signal distribution within QD-incubated cornea with intact epithelium (left) and with the epithelium removed (right).

([CdSe] = 12.5, 25, and 50 μM). Each plate was incubated for 24 or 48 h for MTT cell viability assay.

MTT Cell Viability Assay. MTT assay was used to evaluate cell viability following QD treatment for 24 or 48 h. Culture medium containing QDs was removed from the cell culture wells, and 200 μL of 0.5 mg/mL MTT (Sigma-Aldrich, St Louis, MO) in DMEM was then added to each well. Cells were returned to the incubator for 3 h. At the end of incubation, the medium was removed, and the cells were rinsed by 200 μL of PBS for 1 min. PBS was removed by aspiration, and 200 μL of DMSO was added to each well and incubated for 15 min on a rotating platform in order to dissolve MTT. Microplates were read at the wavelength of 550 nm in a Multiskan microplate with Ascent Software (BIO-RED Model 680, Philadelphia USA). The data of QD-treated samples was derived by subtracting the average background absorbance from control wells (DMEM only) and was expressed as a percentage of vehicle-treated control groups. Three replicates per data point were used for all treatments.

Measurement of QD Uptake Using Flow Cytometry. BCF suspension (100 μL) of 106 cells/mL in DMEM medium was added to each tube to obtain final QD concentrations of 5, 10, and 20 nM. The samples were then incubated at room temperature for 25 min. At the end of incubation, the samples were placed on ice in order to stop the process of endocytosis. Ice-cold PBS (800 μL) was added to each sample and then sent for flow cytometry analysis (EPICS XL-MCL flow cytometer, Coulter, USA). Flow cytometric analysis of BCF provided FSC/SSC dot plots of a population corresponding to endocytosis. A gating strategy was used to acquire 10,000 cells per sample at a rate of 150 cells/s. Fluorescence histograms represented the relative fluorescence on a logarithmic scale. The mean of fluorscent intensity represented the quantity of endocytic QDs within BCF.

Statistical Analysis of Data. All graphs were constructed using Origin 6.0 Professional. The *P* test was used to compare the effect of QD surface coatings, concentrations, incubation period, and cell sources on QD−cell interactions. All statistical analyses were performed using Origin 6.0 Professional. Significance for all values was set at $p < 0.05$.

RESULTS AND DISCUSSION

Permeability and Distribution of QDs through the Cornea. The permeability of QDs to the cornea was first determined using an in vitro bovine model. A home-built two-photon microscopic system was used for noninvasive corneal imaging. The two-photon fluorescent signals were collected from both QDs and cellular structures for the intrinsic fluorescent components such as NAD(P)H, while the SHG signals were derived from a noncentrosymmetrical collagenous structure, which was the major structural component within the corneal stroma. QDs prepared with different functional groups (QD-PEG, QD-NH_2, and QD-COOH) were tested for the permeability into intact cornea using a flow-through diffusion system, and the results showed that QDs were all limited within the layer of epithelium with an incubation time up to 3 h (data not shown in detail). The penetration depth of QDs was limited within the depth of 20 μm from the surface, within the layer of epithelium, following an incubation period of 80 min (the period of 80 min was chosen because a steady stage was achieved following testing) (Figure 1). However, once the epithelium was removed, QDs penetrated into the corneal stromal layer (Figure 1). Furthermore, we found that those penetration profiles were similar and that the penetration depths were close to 200 μm for all three samples (QD-PEG, QD-NH_2, and QD-COOH). The distribution of QDs within the stroma followed a significant concentration gradient, with the intensity of fluorescent signals decayed increasing as the imaging depth increased, which therefore implied that the distribution of QDs within the cornea followed an order of passive diffusion.

The three-dimensional localization of QDs within the cornea was further demonstrated by two-photon imaging (Figure 2). In the normal cornea, epithelial cells were visualized by cytoplasmic autofluorescence, while stromal collagen was characterized by SHG signals (Figure 2, left). In QD-treated cornea with intact epithelium, the fluorescent signals increased inhomogenously within the epithelium due to the presence of QDs within the cytoplasm, while the stroma was free of fluorescent QDs (Figure 2, middle). However, in the cornea with the autofluorescent epithelium removed, fluorescent signals were detected within the SHG-generating collagenous stroma (Figure 2, right). The fluorescent QDs diffused three-dimensionally within the hydrophilic collagenous stroma, following a concentration gradient from the surface. The fluorescent QD particles could be detected up to the depth of 200 μm. The distribution of QDs within the stroma also followed a paralleled layered pattern, interlaced by SHG-generating collagenous lamellae, which was the characteristic architecture of the corneal stroma. It therefore implied that most QDs localized within the interlamellar spaces of the hydrophilic collagenous stroma.

Moreover, we found that QDs localized not only within the interfibrillar space (Figure 3a) but also within the cells (Figure 3b) of the corneal stroma. This result therefore showed that the epithelium of the cornea played an important role in preventing the penetration of QDs. But once the barrier was destroyed, QDs may penetrate and reside within both the intracellular and extracellular spaces of the hydrophilic corneal stroma.

dx.doi.org/10.1021/tx100376n |*Chem. Res. Toxicol.* 2011, 24, 253–261

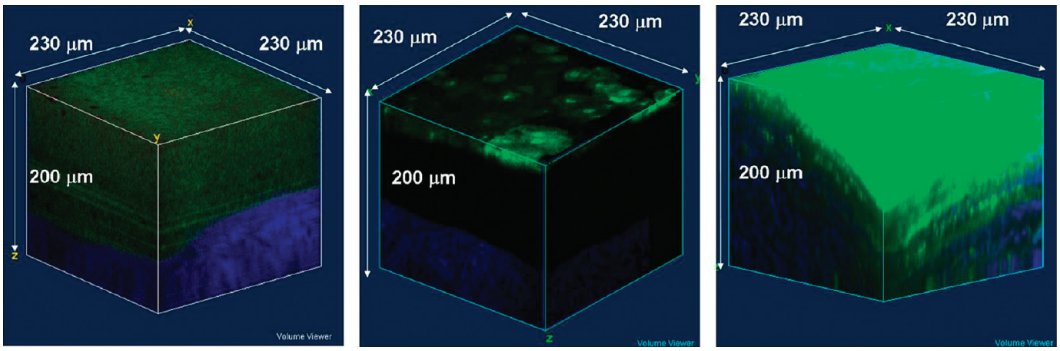

Figure 2. Two-photon 3D imaging of intact bovine cornea without QD incubation (left), intact cornea with QD incubation (middle), and denuded cornea with QD incubation (right). Pseudogreen color, fluorescent signals; pseudoblue color, second harmonic generation signals.

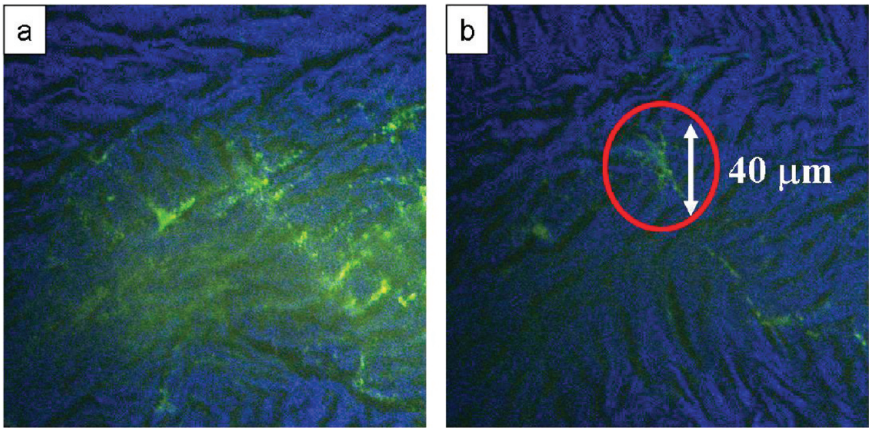

Figure 3. Two-photon imaging of QD-incubated denuded cornea at the depth of 92 and 126 μm from the surface. Fluorescent QDs localized both within the interfibrillar space (a) and within the cells as indicated by the red circle (b) in the corneal stroma. Image size, 230 μm · 230 μm; pseudogreen color, fluorescent signals; pseudoblue color, second harmonic generation signals.

Similar permeability experiments have been done in the porcine skin model before since that skin, the largest organ of the body, was the major potential route of exposure to nanoparticles for both producers and consumers.[36] QD565 with three different surface coatings (QD-PEG, QD-COOH, and QD-NH_2) have been demonstrated to penetrate the stratum corneum and localize within the epidermal and dermal layer during an incubation period of 8 h, the span of one day of working hours, while QD655 coated with PEG and NH_2 was localized within epidermal layers after 8 h, and QD655 coated with the COOH group did not penetrate into the stratum corneum until 24 h. It showed that QDs with different physicochemical properties (size, shape, and surface coating) can penetrate intact skin within the span of one day of working hours. The cornea, just like skin, was known to exhibit poor permeability to hydrophilic molecules.[55] The barrier properties of skin is mainly determined by the stratum corneum, which exhibits low permeability to hydrophilic compounds.[56] In the cornea, the tight junctions between the corneal epithelial cells provide the major barrier for most substances except for small hydrophobic molecules. On the contrary, the collagenous stroma may not limit hydrophilic compounds but may be rate-limiting layer for hydrophobic ones. Although hydrophilic QDs were shown to penetrate into skin during incubation for 8−24 h, the span of one day of working hours during an occupational scenario, they may not penetrate the intact cornea during an incubation period up to 3 h. The reason that incubation for 8−24 h was not rational in the corneal model is because of the rapid washout mechanism for the precorneal tear film. Therefore, we tested the QD incubation period theoretically much longer than the tear film retention time and still found no penetration of QDs, which may therefore prove that the cornea with an intact epithelium yields good protection of QD exposure in an occupational scenario. However, once the epithelium barrier was damaged, hydrophilic QDs penetrated and were retained within the corneal stroma. It should be noticed that corneal epithelium injury is one of the most common ophthalmic injuries. Corneal abrasion has been reported to be the cause of 10% of new patient visits to ophthalmic emergency rooms. Minor trauma, foreign body injuries, chemical burns, and contact lenses may all lead to corneal abrasions. As the application of nanotechnology becomes quite common in our daily life, the possibility of nanoparticle penetration into the injured cornea may therefore increase, especially in the population of contact lens wearers.

In Vivo Corneal Bioaccumulation of QDs. The potential of in vivo intracorneal retention of QDs was further investigated. We injected 10 μL of 4 μM QD565-COOH into the corneal stroma of one eye of C57BL/6J mice, injected PBS into the corneal stroma of the other eye, and followed the distribution and accumulation of QDs in vivo using a two-photon microscopic imaging system (Figure 4a). QDs were shown to be localized both within the interfibrillar space and within corneal stromal cells up to 26 days after injection (Figure 4c). A few in vivo animal studies had shown that QDs may systemically distribute and accumulate in various untargeted organs and tissues such as

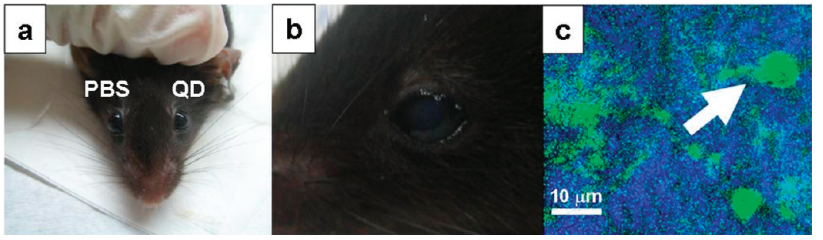

Figure 4. (a) In vivo external photographs of mice corneas following an intrastromal injection of PBS (right eye) and QDs (left eye). (b) The magnified image of the left eye. (c) Two-photon imaging of mice corneas 26 days following intrastromal QD injection. The arrow indicates the intracytoplasmic localized QDs.

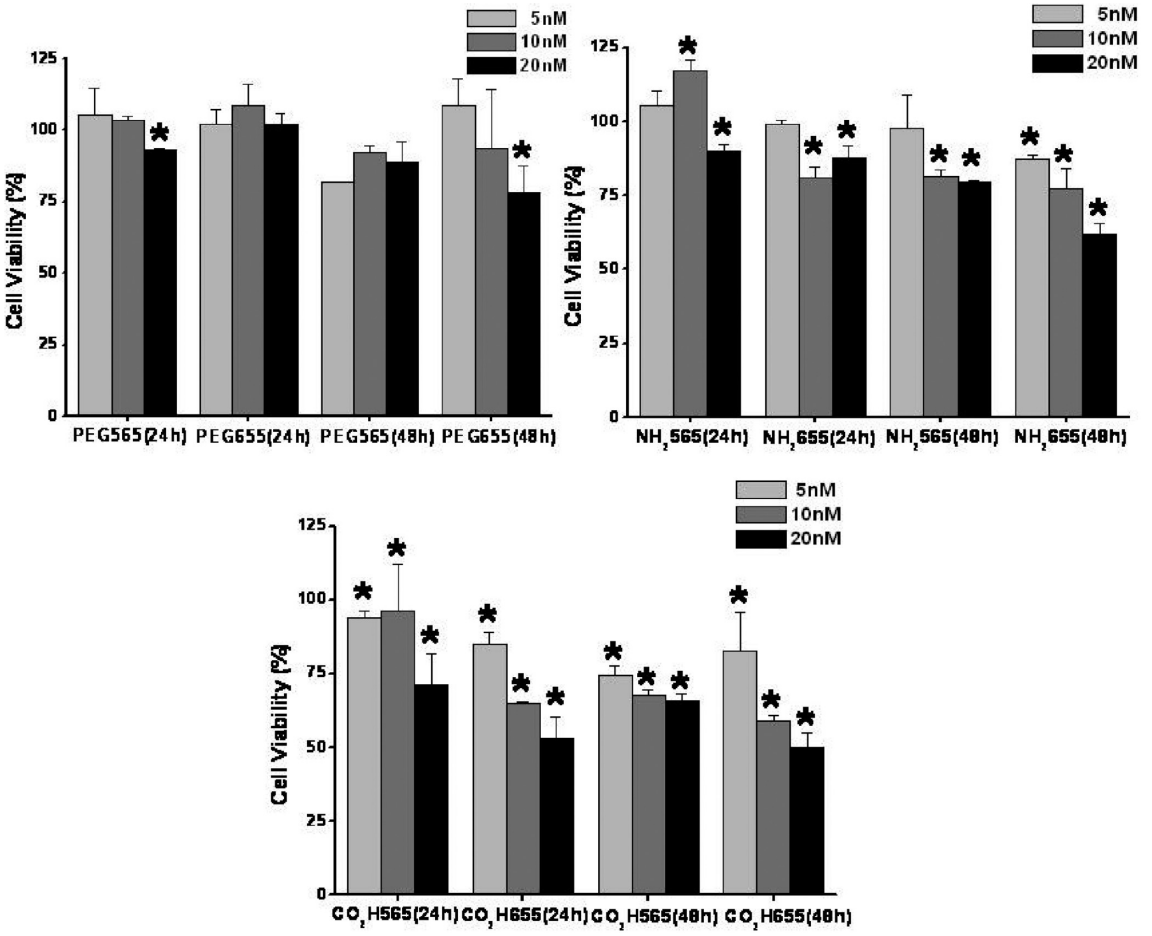

Figure 5. Cell viability of QD-corneal fibroblast using MTT assays. *, significant compared to the control (bovine cornea fibroblast incubated without QDs). Significance was set at $p < 0.05$.

the kidney, liver, lung, spleen, lymph nodes, and bone marrow 1−133 days following intravenous injections. Akerman et al. showed that peptide-coated CdSe/ZnS QDs accumulated in the liver and spleen with no sign of acute toxicity 24 h after intravenous injection in a BALBc mice model.[23] Ballou et al. showed that QDs remained in the liver, lymph nodes, and bone marrow for a month after injection, while the distribution was similar to what was observed 24 h after injection, and the effect was found to be varied with the surface coatings.[26] Fischer et al. also found that QDs were retained in the spleen, kidney, and bone marrow without being cleared away 10 days after injection.[28] We herein demonstrated that hydrophilic QDs accumulated in the cornea in vivo 26 days after intracorneal injection. Although the stroma and endothelium were not dominant barriers like the epithelium and provided only barriers for lipophilic molecules, hydrophilic QDs were found not to be cleared away from the hydrophilic corneal stroma up to a relatively long period of 26 days. As the clearance is an important process for the safety of nanotoxicity, it may imply the potential toxicity resulting from QD bioaccumulation within the cornea.

Cytotoxicity of QDs in Vitro. Now, we have shown that QDs may penetrate into the cornea under the condition of the epithelium barrier being injured and might be retained within the corneal stroma both intracellularly and extracellularly up to 26 days after injection. We therefore further evaluated the potential cytotoxicity of QD bioaccumulation within the cornea. The interactions

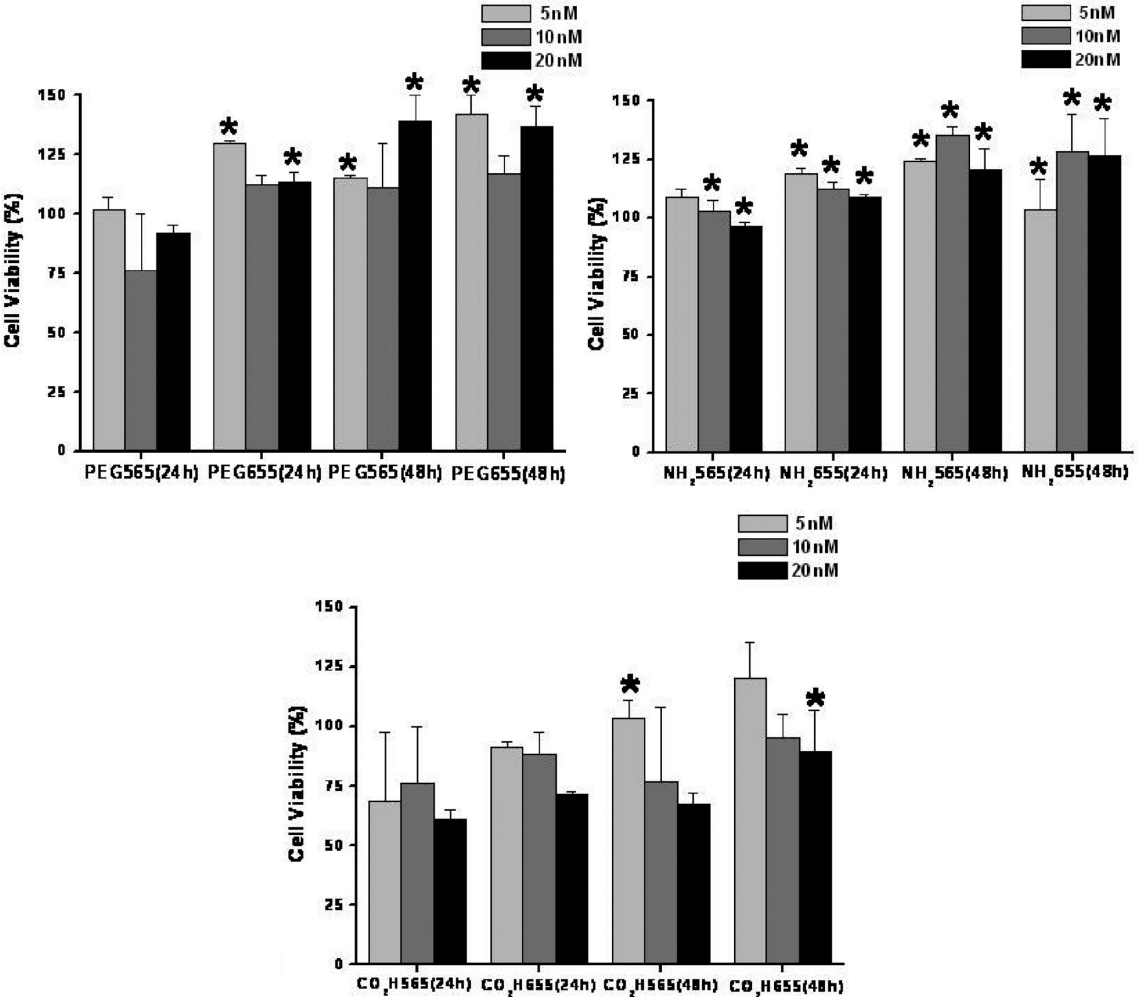

Figure 6. Cell viability of QD-skin fibroblast using MTT assays. *, significant compared to the control (bovine skin fibroblast incubated without QDs). Significance was set at $p < 0.05$.

of QDs with bovine corneal fibroblasts (BCF) in an in vitro model and the physicochemical parameters that might affect the interactions were investigated. The MTT assay was used to evaluate the viability of BCF incubated with 6 different QDs (QD565-PEG, QD565-NH_2, QD565-COOH, QD655-PEG, QD655-NH_2, and QD655-COOH) in three different concentrations of 5, 10, 20 nM for 24 and 48 h (Figure 5). Bovine skin fibroblasts (BSF) were also treated with the same protocol in order to demonstrate the potential difference in susceptibility for QD toxicity. No statistically significant effect on BCF viability under 5 nM QD565-PEG, QD565-NH_2, QD655-PEG, and QD655-NH_2 treatment for 24 h, and QD565-PEG, QD565-NH_2, and QD655-PEG treatment for 48 h was observed. In addition, a mild decrease (6−25.6%) in cell viability was seen in QD treatments of 5 nM QD565-COOH and QD655-COOH treated for 24 h, and QD565-COOH, QD655-NH_2, and QD655-COOH treated for 48 h. Briefly, under low QD concentration (5 nM) treatment, the cell viability of BCF was not affected or mildly affected. As the concentration and incubation period increased, the effect of cytotoxicity increased with 50% decrease of cell viability in maximum in the high concentration (20 nM) QD655-COOH group with a 48-h incubation period (Figure 5). In addition, there was a statistically significant difference in the influence of the decrease of cell viability between QDs with different functional groups (COOH > NH_2 > PEG). In the QD-PEG group, there was no significant decrease in BCF cell viability except for the high concentration (20 nM) group of QD565 treated for 24 h and QD655 for 48 h. However, in the QD-COOH group, BCF cell viability was decreased significantly in treatments of all concentrations and incubation periods (3.8−50%). Similar time-, concentration-, and functional group-dependent effects in the cell viability of QDs were observed in the BSF system (Figure 6). However, BCF was shown to be more susceptible to QDs than BSF (data not shown in detail), which therefore implied the difference in susceptibility among cell types. Environmental factors and physicochemical properties of QDs have been proven to influence the QD−cell interactions in many different cell types in the in vitro model. Derfus et al. have found that the ZnS shell reduced the cytotoxic effect of CdSe QDs, which resulted from the oxidation of the core in the rat primary hepatocyte culture system.[46] Shiohara et al. have demonstrated a concentration-dependent cytotoxic effect in three different MUA-coated CdSe/ZnS QDs in three different cell lines (Vero cells, Hela cells, and human primary hepatocytes),[45] while Selvan et al. have also found a similar dose-dependent tendency in SiO_2, mercaptoacetic acid, and polyanhydride surface-coated CdSe/ZnS QDs in three different cell lines (human liver carcinoma, NIH T3T cells, and COS-7 cells).[47] Surface coatings had also

been shown to influence the cytotoxicity of QDs. ZnS capping and SiO_2 coating were proven to provide protection against CdSe dissolution in Selvan's study. Ryman-Rasmussen et al. had observed a 40% decrease in human epidermal keratinocyte viability when treated with 20 nM QD-COOH for 24 h but not for the QD-PEG and QD-NH_2 groups.[49] Furthermore, an additional 30% decrease in cell viability was observed with incubation for 48 h in the QD-COOH group, which therefore implied a time-dependent tendency of QD cytotoxicity. In this work, we demonstrated a similar time-, concentration-, and functional group-dependent effect of QDs on BCF viability. Notice that BCF viability can be affected and decreased up to 50% in a relatively short duration (48 h) in 20 nM QD655-COOH, while QDs were proven to be able to be retained within the cornea in vivo for a much longer duration than that. We may therefore propose the potential of QD cytotoxicity in the cornea.

QD Uptake in the BCF. We also evaluated the impact of functional groups, QD concentration, and incubation period on QD uptake in the BCF in vitro culture system. There was a significantly higher percentage of intracytoplasmic localization of QDs observed in the QD-COOH group (90%) as compared with the QD-PEG (40%) and QD-NH_2 (50%) groups by confocal microscopic imaging, which was similar to the results demonstrated in epidermal keratinocytes. The intracytoplasmic localization of QDs may cause cell apoptosis.[57−59] We also quantified the percentage of endocytosis in the QD-COOH group with different QD concentrations (5 nM, 10 nM, and 20 nM) and incubation periods (24 and 48 h) by flow cytometry. A significant dose-dependent tendency of QD uptake was seen. By 24 h, a 3.6-fold increase in QD uptake was noted in 20 nM compared with that in 5 nM, and a less significant time-dependent trend of QD uptake was seen as the efficacy of endocytosis was minimally increased by 48 h (3, 12, and 17% increase in 5, 10, and 20 nM, respectively). Briefly, we demonstrated that QD uptake in the BCF system was also time-, concentration-, and functional group-dependent, which was parallel to the effects in QD cytotoxicity. As Chang et al. have pointed out that cytotoxicity was similar between the differently coated QDs when the intracellular concentration was the same,[29] we may therefore hypothesize that the magnitude of cytotoxicity was correlated to the efficacy of intracellular QD uptake, which was time-, concentration-, coating-dependent.

CONCLUSIONS

In conclusion, we have demonstrated that untargeted hydrophilic QDs may penetrate and be retained within the cornea for a relatively long period while the epithelium is injured, using a noninvasive two-photon imaging system. We have also shown that QDs can affect corneal stromal cell viability up to a significant magnitude of 50%, under a relatively low concentration (20 nM) and short duration (48 h), while QDs were proven to accumulate within the cornea in vivo for a much longer duration than that (26 days). Since corneal stromal cells are crucial for the maintenance of the health and transparency of the cornea, the potential QD cytotoxicity due to bioaccumulation may be a major concern because of the threat to corneal health. Furthermore, as the applications of nanoparticles has increased vigorously recently (including UV-blocking agents, cosmetics, etc.), and corneal abrasion is truly not an uncommon situation in our daily lives, especially for the large population of contact lens wearers, it is definitely worthwhile for us to pay more attention to preventing the potential risk of corneal exposure to nanoparticles.

AUTHOR INFORMATION

Corresponding Author

*E-mail: cjchen@ntnu.edu.tw (C.-C. C.) and b0401018@cgmh.org.tw (H.-Y. T.).

Funding Sources

This work was supported by NSC-98-3114-M-003-001, IAMS, and NTNU.

ACKNOWLEDGMENT

We thank National Taiwan Normal University, National Taiwan University, and Chang-Gung Memorial Hospital for providing experimental equipment.

REFERENCES

(1) Lewinski, N., Colvin, V., and Drezek, R. (2008) Cytotoxicity of nanoparticles. *Small 4*, 26–49.

(2) Hardman, R. (2006) A toxicologic review of quantum dots: Toxicity depends on physicochemical and environmental factors. *Environ. Health Perspect. 114*, 165–172.

(3) Elder, A., Yang, H., Gwiazda, R., Teng, X., Thurston, S., He, H., and Oberdorster, G. (2007) Testing nanomaterials of unknown toxicity: An example based on platinum nanoparticles of different shapes. *Adv. Mater. 19*, 3124–3219.

(4) Medintz, I. L., Uyeda, H. T., Goldman, E. R., and Mattoussi, H. (2005) Quantum dot bioconjugates for imaging, labelling and sensing. *Nat. Mater. 4*, 435–446.

(5) Aubin-Tam, M. E., and Hamad-Schifferli, K. (2008) Structure and function of nanoparticle-protein conjugates. *Biomed. Mater.*10.1088/1748-6041/3/3/034001.

(6) Nazzal, A. Y., Wang, X. Y., Qu, L. H., Yu, W., Wang, Y. J., Peng, X. G., and Xiao, M. (2004) Environmental effects on photoluminescence of highly luminescent CdSe and CdSe/ZnS core/shell nanocrystals in polymer thin films. *J. Phys. Chem. B 108*, 5507–5515.

(7) Alivisatos, A. P., Gu, W. W., and Larabell, C. (2005) Quantum dots as cellular probes. *Annu. Rev. Biomed. Eng. 7*, 55–76.

(8) Michalet, X., Pinaud, F. F., Bentolila, L. A., Tsay, J. M., Doose, S., Li, J. J., Sundaresan, G., Wu, A. M., Gambhir, S. S., and Weiss, S. (2005) Quantum dots for live cells, in vivo imaging, and diagnostics. *Science 307*, 538–544.

(9) Mattoussi, H., Mauro, J. M., Goldman, E. R., Anderson, G. P., Sundar, V. C., Mikulec, F. V., and Bawendi, M. G. (2000) Self-assembly of CdSe-ZnS quantum dot bioconjugates using an engineered recombinant protein. *J. Am. Chem. Soc. 122*, 12142–12150.

(10) Freeman, R., Finder, T., Gill, R., and Willner, I. (2010) Probing protein kinase (CK2) and alkaline phosphatase with CdSe/ZnS quantum dots. *Nano Lett. 10*, 2192–2196.

(11) Huang, J., Huang, Z. Q., Yang, Y., Zhu, H. M., and Lian, T. Q. (2010) Multiple exciton dissociation in CdSe quantum dots by ultrafast electron transfer to adsorbed methylene blue. *J. Am. Chem. Soc. 132*, 4858–4864.

(12) Gao, X., Cui, Y., Levenson, R. M., Chung, L. W., and Nie, S. (2004) In vivo cancer targeting and imaging with semiconductor quantum dots. *Nat. Biotechnol. 22*, 969–976.

(13) Larson, D. R., Zipfel, W. R., Williams, R. M., Clark, S. W., Bruchez, M. P., Wise, F. W., and Webb, W. W. (2003) Water-soluble quantum dots for multiphoton fluorescence imaging in vivo. *Science 300*, 1434–1436.

(14) Wamement, M. R., Tomlinson, I. D., Chang, J. C., Schreuder, M. A., Luckabaugh, C. M., and Rosenthal, S. J. (2008) Controlling the reactivity of ampiphilic quantum dots in biological assays through hydrophobic assembly of custom PEG derivatives. *Bioconjugate Chem. 19*, 1404–1413.

(15) Murray, C. B., Kagan, C. R., and Bawendi, M. G. (2000) Synthesis and characterization of monodisperse nanocrystals and close-packed nanocrystal assemblies. *Annu. Rev. Mater. Sci. 30*, 545–610.

(16) Wu, W. T., Aiello, M., Zhou, T., Berliner, A., Banerjee, P., and Zhou, S. Q. (2010) In-situ immobilization of quantum dots in polysaccharide-based nanogels for integration of optical pH-sensing, tumor cell imaging, and drug delivery. *Biomaterials 31*, 3023–3031.

(17) Ozkan, M. (2004) Quantum dots and other nanoparticles: what can they offer to drug discovery?. *Drug Discovery Today 9*, 1065–1071.

(18) Hauck, T. S., Anderson, R. E., Fischer, H. C., Newbigging, S., and Chan, W. C. (2010) In vivo quantum-dot toxicity assessment. *Small 6*, 138–144.

(19) Braydich-Stolle, L., Hussain, S., Schlager, J. J., and Hofmann, M. C. (2005) In vitro cytotoxicity of nanoparticles in mammalian germline stem cells. *J. Toxicol. Sci. 88*, 412–419.

(20) Wang, L., Nagesha, D. K., Selvarasah, S., Dokmeci, M. R., and Carrier, R. L. (2008) Toxicity of CdSe nanoparticles in caco-2 cell cultures. *J. Nanobiotechnol. 6*, 11.

(21) Chen, F. Q., and Gerion, D. (2004) Fluorescent CdSe/ZnS nanocrystal-peptide conjugates for long-term, nontoxic imaging and nuclear targeting in living cells. *Nano Lett. 4*, 1827–1832.

(22) Jacobsen, N. R., Moller, P., Jensen, K. A., Vogel, U., Ladefoged, O., Loft, S., and Wallin, H. (2009) Lung inflammation and genotoxicity following pulmonary exposure to nanoparticles in ApoE−/− mice. *Part. Fibre Toxicol. 6*, 1–17.

(23) Akerman, M. E., Chan, W. C., Laakkonen, P., Bhatia, S. N., and Ruoslahti, E. (2002) Nanocrystal targeting in vivo. *Proc. Natl. Acad. Sci. U.S.A. 99*, 12617–12621.

(24) Chen, J. Y., Zhou, H. J., Santulli, A. C., and Wong, S. S. (2010) Evaluating cytotoxicity and cellular uptake from the presence of variously processed TiO2 nanostructured morphologies. *Chem. Res. Toxicol. 23*, 871–879.

(25) Tao, Z. M., Toms, B. B., Goodisman, J., and Asefa, T. (2009) Mesoporosity and functional group dependent endocytosis and cytotoxicity of silica nanomaterials. *Chem. Res. Toxicol. 22*, 1869–1880.

(26) Ballou, B., Lagerholm, B. C., Ernst, L. A., Bruchez, M. P., and Waggoner, A. S. (2004) Noninvasive imaging of quantum dots in mice. *Bioconjugate Chem. 15*, 79–86.

(27) Oberdorster, G., Oberdorster, E., and Oberdorster, J. (2005) Nanotoxicology: An emerging discipline evolving from studies of ultrafine particles. *Environ. Health Perspect. 113*, 823–839.

(28) Fischer, H. C., Liu, L. C., Pang, K. S., and Chan, W. C. W. (2006) Pharmacokinetics of nanoscale quantum dots: In vivo distribution, sequestration, and clearance in the rat. *Adv. Funct. Mater. 16*, 1299–1305.

(29) Chang, E., Thekkek, N., Yu, W. W., Colvin, V. L., and Drezek, R. (2006) Evaluation of quantum dot cytotoxicity based on intracellular uptake. *Small 2*, 1412–1417.

(30) Hoshino, A., Hanaki, K., Suzuki, K., and Yamamoto, K. (2004) Applications of T-lymphoma labeled with fluorescent quantum dots to cell tracing markers in mouse body. *Biochem. Biophys. Res. Commun. 314*, 46–53.

(31) Hsieh, S. C., Wang, F. F., Lin, C. S., Chen, Y. J., Hung, S. C., and Wang, Y. J. (2006) The inhibition of osteogenesis with human bone marrow mesenchymal stem cells by CdSe/ZnS quantum dot labels. *Biomaterials 27*, 1656–1664.

(32) Baroli, B. (2010) Penetration of nanoplarticles and nanomaterials in the skin: fiction or reality?. *J. Pharm. Sci. 99*, 21–50.

(33) Schneider, M., Stracke, F., Hansen, S., and Schaefer, U. F. (2009) Nanoparticles and their interactions with the dermal barrier. *Dermatoendocrinol 1*, 197–206.

(34) Lee, J. N., Jee, S. H., Chan, C. C., Lo, W., Dong, C. Y., and Lin, S. J. (2008) The effects of depilatory agents as penetration enhancers on human stratum corneum structures. *J. Invest. Dermatol. 128*, 2240–2247.

(35) Kuo, T. R., Wu, C. L., Hsu, C. T., Lo, W., Chiang, S. J., Lin, S. J., Dong, C. Y., and Chen, C. C. (2009) Chemical enhancer induced changes in the mechanisms of transdermal delivery of zinc oxide nanoparticles. *Biomaterials 30*, 3002–3008.

(36) Ryman-Rasmussen, J. P., Riviere, J. E., and Monteiro-Riviere, N. A. (2006) Penetration of intact skin by quantum dots with diverse physicochemical properties. *J. Toxicol. Sci. 91*, 159–165.

(37) Gopee, N. V., Roberts, D. W., Webb, P., Cozart, C. R., Siitonen, P. H., Warbritton, A. R., Yu, W. W., Colvin, V. L., Walker, N. J., and Howard, P. C. (2007) Migration of intradermally injected quantum dots to sentinel organs in mice. *J. Toxicol. Sci. 98*, 249–257.

(38) Delehanty, J. B., Medintz, I. L., Pons, T., Brunel, F. M., Dawson, P. E., and Mattoussi, H. (2006) Self-assembled quantum dot-peptide bioconjugates for selective intracellular delivery. *Bioconjugate Chem. 17*, 920–927.

(39) Choi, A. O., Cho, S. J., Desbarats, J., Lovric, J., and Maysinger, D. (2007) Quantum dot-induced cell death involves Fas upregulation and lipid peroxidation in human neuroblastoma cells. *J. Nanobiotechnol. 5*, 1.

(40) Duan, H. W., and Nie, S. M. (2007) Cell-penetrating quantum dots based on multivalent and endosome-disrupting surface coatings. *J. Am. Chem. Soc. 129*, 3333–3338.

(41) Zhang, T. T., Stilwell, J. L., Gerion, D., Ding, L. H., Elboudwarej, O., Cooke, P. A., Gray, J. W., Alivisatos, A. P., and Chen, F. F. (2006) Cellular effect of high doses of silica-coated quantum dot profiled with high throughput gene expression analysis and high content cellomics measurements. *Nano Lett. 6*, 800–808.

(42) Jaiswal, J. K., Mattoussi, H., Mauro, J. M., and Simon, S. M. (2003) Long-term multiple color imaging of live cells using quantum dot bioconjugates. *Nat. Biotechnol. 21*, 47–51.

(43) Dubertret, B., Skourides, P., Norris, D. J., Noireaux, V., Brivanlou, A. H., and Libchaber, A. (2002) In vivo imaging of quantum dots encapsulated in phospholipid micelles. *Science 298*, 1759–1762.

(44) Hanaki, K., Momo, A., Oku, T., Komoto, A., Maenosono, S., Yamaguchi, Y., and Yamamoto, K. (2003) Semiconductor quantum dot/albumin complex is a long-life and highly photostable endosome marker. *Biochem. Biophys. Res. Commun. 302*, 496–501.

(45) Shiohara, A., Hoshino, A., Hanaki, K., Suzuki, K., and Yamamoto, K. (2004) On the cyto-toxicity caused by quantum dots. *Microbiol. Immunol. 48*, 669–675.

(46) Derfus, A. M., Chan, W. C. W., and Bhatia, S. N. (2004) Probing the cytotoxicity of semiconductor quantum dots. *Nano Lett. 4*, 11–18.

(47) Selvan, S. T., Tan, T. T., and Ying, J. Y. (2005) Robust, non-cytotoxic, silica-coated CdSe quantum dots with efficient photoluminescence. *Adv. Mater. 17*, 1620–1625.

(48) Kirchner, C., Liedl, T., Kudera, S., Pellegrino, T., Javier, A. M., Gaub, H. E., Stolzle, S., Fertig, N., and Parak, W. J. (2005) Cytotoxicity of colloidal CdSe and CdSe/ZnS nanoparticles. *Nano Lett. 5*, 331–338.

(49) Ryman-Rasmussen, J. P., Riviere, J. E., and Monteiro-Riviere, N. A. (2007) Surface coatings determine cytotoxicity and irritation potential of quantum dot nanoparticles in epidermal keratinocytes. *J. Invest. Dermatol. 127*, 143–153.

(50) Basu, S., Cunningham, L. P., Pins, G. D., Bush, K. A., Taboada, R., Howell, A. R., Wang, J., and Campagnola, P. J. (2005) Multiphoton excited fabrication of collagen matrixes cross-linked by a modified benzophenone dimer: Bioactivity and enzymatic degradation. *Biomacromolecules 6*, 1465–1474.

(51) Denk, W., Strickler, J. H., and Webb, W. W. (1990) 2-Photon laser scanning fluorescence microscopy. *Science 248*, 73–76.

(52) Piston, D. W., Masters, B. R., and Webb, W. W. (1995) 3-dimensionally resolved NAD(P)H cellular metabolic redox imaging of the in-situ cornea with 2-photon excitation laser-scanning microscopy. *J. Microsc. 178*, 20–27.

(53) Yeh, A. T., Nassif, N., Zoumi, A., and Tromberg, B. J. (2002) Selective corneal imaging using combined second-harmonic generation and two-photon excited fluorescence. *Opt. Lett. 27*, 2082–2084.

(54) Teng, S. W., Tan, H. Y., Peng, J. L., Lin, H. H., Kim, K. H., Lo, W., Sun, Y., Lin, W. C., Lin, S. J., Jee, S. H., So, P. T. C., and Dong, C. Y. (2006) Multiphoton autofluorescence and second-harmonic generation imaging of the ex vivo porcine eye. *Invest. Ophthalmol. Vis. Sci. 47*, 1216–1224.

(55) Prausnitz, M. R., and Noonan, J. S. (1998) Permeability of cornea, sclera, and conjunctiva: a literature analysis for drug delivery to the eye. *J. Pharm. Sci. 87*, 1479–1488.

(56) Mitragotri, S. (2003) Modeling skin permeability to hydrophilic and hydrophobic solutes based on four permeation pathways. *J. Controlled Release 86*, 69–92.

(57) Kang, B., Mackey, M. A., and El-Sayed, M. A. (2010) Nuclear targeting of gold nanoparticles in cancer cells induces DNA damage, causing cytokinesis arrest and apoptosis. *J. Am. Chem. Soc. 132*, 1517–1519.

(58) Chan, W. H., Shiao, N. H., and Lu, P. Z. (2006) CdSe quantum dots induce apoptosis in human neuroblastoma cells via mitochondrial-dependent pathways and inhibition of survival signals. *Toxicol. Lett. 167*, 191–200.

(59) Park, E. J., Yi, J., Chung, Y. H., Ryu, D. Y., Choi, J., and Park, K. (2008) Oxidative stress and apoptosis induced by titanium dioxide nanoparticles in cultured BEAS-2B cells. *Toxicol. Lett. 180*, 222–229.